Membrane and Water Treatment, *Vol. 11*, *No. 4 (2020) 275-282*
DOI: https://doi.org/10.12989/mwt.2020.11.4.275

Wastewater treatment using a hybrid process coupling adsorption on marl and microfiltration

Bakhta Maimoun[1], Abderrahmane Djafer[1], Lahcène Djafer[1], Rose-Marie Marin-Ayral[2] and André Ayral*[3]

[1]*Laboratoire Eau et Environnement, Hassiba Benbouali University, Chlef, Algeria*
[2]*Institut Charles Gerhardt Montpellier, Univ Montpellier, Montpellier, France*
[3]*Institut Européen des Membranes, Univ Montpellier, Montpellier, France*

(Received September 7, 2019, Revised April 11, 2020, Accepted April 16, 2020)

Abstract. Hranfa's marl, a local natural mineral, is selected for the decontamination by adsorption of aqueous effluents in textile industry. Its physicochemical characterization is first performed. It is composed mainly of Calcite, Quartz, Ankerite and Muscovite. Its specific surface area is 40 m^2 g^{-1}. Its adsorption performance is then tested in batch conditions using an industrial organic dye, Bemacid Red E-TL, as a model pollutant. The measured adsorption capacity of Hranfa's marl is 16 mg g^{-1} which is comparable to that of other types of natural adsorbents. A hybrid process is tested coupling adsorption of the dye on marl in suspension and microfiltration. An adsorption reactor is inserted into the circulation loop of a microfiltration pilot using ceramic membranes. This makes possible a continuous extraction of the treated water provided that a periodic replacement of the saturated adsorbent is done. The breakthrough curve obtained by analyzing the dye concentration in the permeate is close to the ideal one considering that no dye will cross the membrane as long as the adsorbent load is not saturated. These first experimental data provide proof of concept for such a hybrid process.

Keywords: hybrid process, microfiltration by ceramic membrane, natural adsorbents, wastewater treatment

1. Introduction

Water is essential to life and to any socio-economic activity, whatever the level of development. Its excessive consumption for manufacturing finished products by many industries (textiles, paper, chemicals, plastics, metals, microelectronics, food processing, etc.) generates huge amounts of wastewater containing complex mixtures of pollutants. As an example, the overall global production of wastewater was estimated to be 450 km^3 per year in 2010, approximately 30 % of which was accounted for by the industrial sector (Flörke *et al.* 2013).

Industrial wastewaters containing dyes and/or heavy metals are too often rejected in the environment without any prior treatment. The presence of dyes in these effluents constitutes a danger to human health and the environment because of their stability and their recalcitrant power, which make them toxic and carcinogenic (Djafer *et al.* 2017, Charumathi and Das 2012).

The dye removal from industrial effluents can be done by implementing biological, physical and/or chemical techniques such as electrolysis, chemical precipitation, membrane filtration, reverse osmosis, ion exchange, activated sludge, coagulation flocculation and adsorption on activated carbons (Perineau *et al.* 1983, Yang *et al.* 1988, Fu and Viraraghavan 2001). Adsorption processes implementing activated carbons are currently the most commonly used. However, activated carbons, in the form of powders or granules, are rather expensive adsorbents (current market price of ~ 1 € kg^{-1}).

Efforts are currently oriented towards low cost adsorption processes using biosourced or natural mineral materials such as algae, wool waste, agricultural waste (corn ear, hulls of nuts, rice husk etc.), chitin, chitosan or zeolites and clays (bentonite, kaolinite etc.). Compared to activated carbons, these natural adsorbents have shown rather good efficiency for the removal of pollutants from industrial effluents, especially for heavy metals and dyes (Reddad *et al.* 2004, Dali-Youcef *et al.* 2006, Cimino *et al.* 2000, Vaughan *et al.* 2001, Baghriche *et al.* 2008, Bagane and Guiza 2000).

This work is part of a project to exploit different local clay minerals (marls, bentonites, kaolinites) for the decontamination by physisorption of industrial aqueous effluents containing pollutants like organic dyes or heavy metals. The basic idea is to select low cost and abundant natural adsorbents even if their adsorption performance is poor compared to advanced synthetic materials, and to favor their storage after use rather than their regeneration. Due to its abundance, a local marl has been selected here, namely Hranfa's marl. Its physicochemical characterization was first performed. Its adsorption performance was then tested in batch conditions using an industrial organic dye, Bemacid Red E-TL, as a model pollutant. In view of its future technological use in simple and robust conditions, it was finally implemented in a hybrid process coupling adsorption and membrane separation. To this end, the

*Corresponding author, Professor
E-mail: andre.ayral@umontpellier.fr

ISSN: 2005-8624 (Print), 2092-7037 (Online)

adsorption reactor with marl in suspension was inserted into the circulation loop of a microfiltration pilot using ceramic membranes, for a continuous extraction of the treated water.

2. Materials and methods

2.1 Materials

The diatomaceous marl of Jebel Dhahra in Hranfa (30 km north-west of Chlef, Algeria) used as adsorbent was first crushed and then sieved in a shaker brand of type Retsch-5657 Haan equipped with a series of sieves. The fraction 80-100 µm was selected for the adsorption tests.

The tested industrial dye was Bemacid Red E-TL (CHT 2019). It belongs to the category of water-soluble anionic dyes and was provided by the artificial silk production company EATIT, in Tlemcen (Algeria). A stock solution was prepared by dissolving 1000 mg of dye per liter of double distilled water. From this stock solution, diluted solutions were prepared to carry out different experiments in batch conditions or in the hybrid pilot unit.

2.2 Physicochemical characterization of Hranfa's marl

The morphological analysis and the elemental chemical composition of the marl were investigated using a Scanning Electron Microscope (SEM) of type Zeiss EVO HD15 equipped with an X-ray energy dispersion (EDX) spectrometer of type Oxford Instruments X-Max N SDD.

The specific surface area was measured by N_2 adsorption at the liquid nitrogen temperature and by applying the Brunauer–Emmett–Teller (BET) method, thanks to an ASAP-2020 Micromeritics apparatus.

The identification of the main crystalline phases constituting the marl was carried out thanks to a X-ray diffractometer of type Malvern Panalytical X-Pert PRO using the monochromatic radiation Kα, Cu = 1.5418 Å, with 2θ varying from 3 to 80° and a step of 0.017°. The Fourier Transform InfraRed (FTIR) spectrum was recorded in transmission mode with powder dispersed in a KBr pellet, and using a spectrometer of type Bruker Tensor 27.

The thermogravimetric analyses (TGA) were done using an apparatus of type TA Instruments SDT 2960.

The turbidity of the marl suspensions was measured using a turbidimeter Lovibond.

2.3 Adsorption measurements in batch conditions

The batch study was carried in 500 mL Erlenmeyer flasks containing 200 mL of solution with various dye concentrations (20-180 mg L^{-1}).The marl was dispersed under stirring with content in suspension ranging from 0.5 to 3.0 g L^{-1}. The effect of pH on the dye removal was studied in a range from 2 to 10 by adjusting the suspension pH with 0.1 M HCl or 0.1 M NaOH solutions. The pH measurements were conducted using a HANNA 120 pH-meter.

The reactor was put on a rotary shaker at a constant speed of 300 rpm under controlled temperature ranging from 15 to 45 °C thanks to the use of a thermostatically-controlled water bath.

Aliquots were periodically taken and centrifuged at 3000 rpm for 5 min. The supernatant liquid was used for measuring the residual dye concentration in solution thanks to the measurement of the absorbance at λ = 508 nm with a UV-Vis spectrophotometer Shimadzu UV-1280.

2.4 Hybrid process coupling adsorption and membrane separation

The schematic representation of the pilot used for these experiments is given in Fig. 1.

A feed tank containing 14 L of dye solution was connected with an adsorption reactor of 11 L stirred with a mechanical agitator Ika RW16 Basic, rotating at ~ 200 rpm. For experiments with adsorbent, 80 g of marl were dispersed in this adsorption reactor. The mixing was good enough for considering the reactor as perfectly agitated. All these experiments were done at 20 ± 2 °C. The overflow of the reactor was poured in the loop of a filtration unit of type Minipilot Orelis Environnement equipped with a single channel tubular alumina microfiltration membrane Microkleansep ™ (Φ_{int} = 0.6 cm, L = 40 cm, filtration area = 0.007162 m^2, average pore size of the separative layer = 0.1 µm). This membrane was selected in order to retain the micron-sized elemental particles resulting from the progressive attrition of the marl aggregates. The total volume of liquid into the loop was equal to 8 L. The transmembrane pressure was fixed at 0.5 bar and the circulation rate was maintained at ~ 1 m/s. The permeate was collected in a permeate tank whereas the retentate was reinjected in the bottom of the adsorption reactor. The flow from the feed tank to the adsorption reactor was controlled to be as close as possible to the outgoing permeate flow (in the range from 20 to 25 mL min^{-1}).

It must be here noted that tests of repeatability done both for batch and hybrid process experiments did not evidence significant differences (in the same order as the experimental uncertainties materialized by the error bars reported in the different figures).

3. Results and discussion

3.1 Physicochemical characterization of Hranfa's marl

The SEM image in Fig. 2 shows a great diversity of morphologies: rounded particles, platelets, needles and also entities with architectural porosity similar to frustules (silica shell) of diatoms. A wide particle size distribution is also observed, ranging from a few µm to several tens of µm despite the initial selection of the particle class [80 – 100 µm]. The divided nature of this marl is also confirmed by a BET surface area equal to 40 m^2 g^{-1} (Table 1). This value is very low compared to that of activated carbons which can exhibit specific surface areas more than 1000 m^2 g^{-1}.

Preliminary tests of sedimentation also confirmed the existence of a significant part of fine particles (micron-sized) showing a low sedimentation velocity (~ 5 10^{-7} m s^{-1}) and

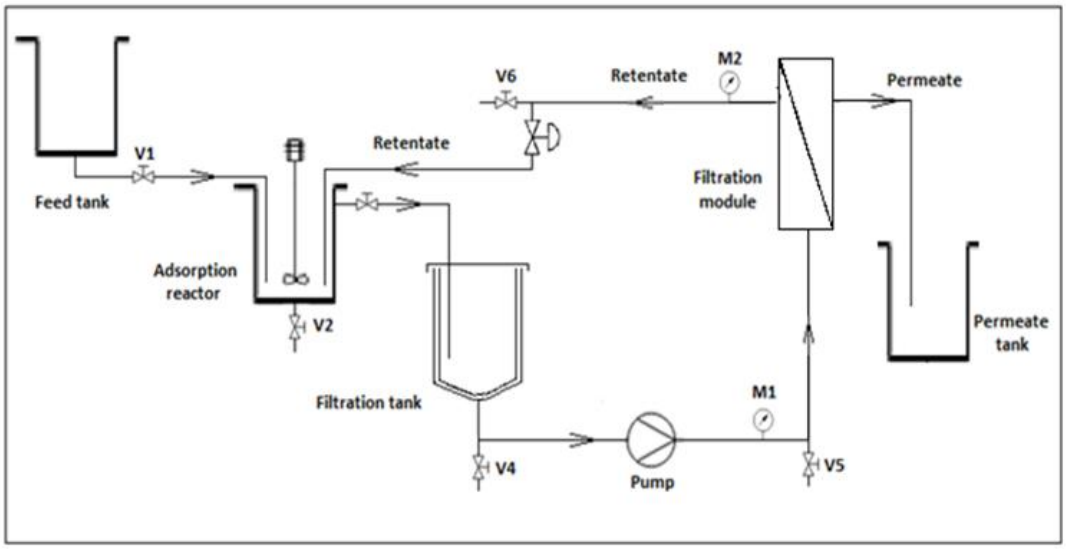

Fig. 1 Schematic of the pilot unit coupling an adsorption reactor and a microfiltration loop equipped with a single-channel tubular ceramic membrane

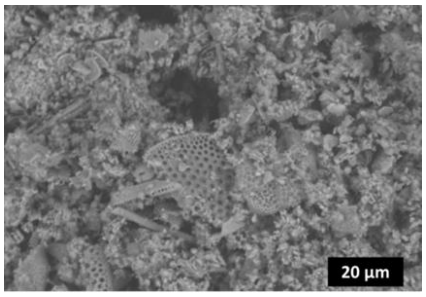

Fig. 2 SEM image of Hranfa's marl

Table 1 Physicochemical characteristics of Hranfa's marl

BET specific surface area (m^2 g^{-1})	Elemental composition from EDX (wt %; ± 1 %)						Weight loss at 900 °C from TGA (wt %; ± 1 %)
	O	Si	Ca	Fe	Al	Mg	
40 ± 1	45	26	18	5	4	2	24

resulting from the easy fragmentation/attrition of larger soft aggregates of marl.

The X-ray pattern of Hranfa's marl is shown in Fig. 3a. The four main crystalline phases are, in descending order of importance, calcium carbonate in the form of Calcite, silica in the form of Quartz, Ankerite (calcium magnesium iron carbonate, $Ca(Fe,Mg,Mn)(CO_3)_2$) and Muscovite, a phyllosilicate of general formula $KAl_2(AlSi_3O_{10})(OH,F)_2$. About this last compound, it must be noted that the identification of the clay phases is very delicate, many clays having very close diffractograms with peak positions varying with chemical composition. Moreover, for the peaks associated with the interlamellar space (in the case of lamellar structures), the position may vary greatly depending on the swelling of the clay. On the other hand, the diatom frustules seen by SEM are composed of amorphous silica.

The FTIR spectrum of Hranfa's marl is given in Fig. 3b. The broad band in the range 3800-3000 cm^{-1} corresponding to stretching of OH groups is mainly due to adsorbed or capillary-condensed molecular water as confirmed by the presence of the band centered at 1645 cm^{-1} and assigned the bending vibration of H_2O. The strong band centered at 1475 cm^{-1} is resulting from the vibration of the carbonate groups present in Calcite and Ankerite. The broad domain of strong absorbance from 1300 cm^{-1} to 400 cm^{-1} is related to vibrations in the different inorganic networks forming Hranfa's marl.

The elemental composition deduced from EDX analyses as well as the weight loss measured by TGA at 900 °C, are in rather good agreement with the different phases identified in the marl (Table 1). Moreover, the preponderance of calcite and a lower content of clay in the used natural mineral are in accordance with its designation as being a marl.

3.2 Adsorption measurements in batch conditions

The adsorption of the dye by the marl increases with time and goes through two distinct stages (Fig. 4a). The initial high rate of removal is due to rapid sorption through the outer surface of the adsorbent. This phenomenon can be explained by the existence of numerous active sorption sites easily accessible to the adsorbate present in the solution (Dinçer *et al.* 2007, Yaneva and Koumanova 2006). A slowing down of the sorption rate to the equilibrium stage can be assigned to a decrease or absence of active sites available on the surface, which causes repulsive forces between the dye molecules fixed on the surface of the adsorbent and the molecules remaining in the solution (Kumar *et al.* 2011). The sorption equilibrium of the dye is attenuated after a stirring time of 20 min associated with an adsorption capacity Q_e = 12.6 mg g^{-1}.

Different kinetics models were tested (pseudo first order, pseudo second order, intraparticle diffusion, Elovich). The best fit was obtained using the pseudo second order model leading to a kinetics constant of 0.243 g mg^{-1} min^{-1}, with a coefficient of determination R^2 equal to 0.999.

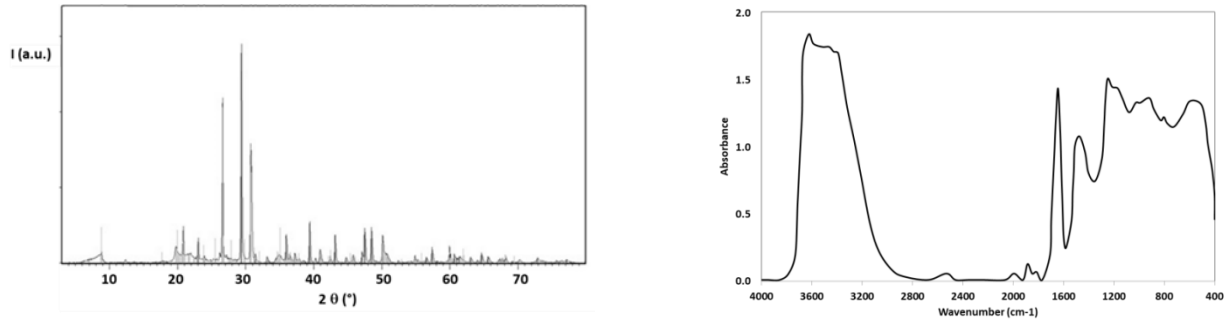

(a) (b)

Fig. 3 XRD pattern (a) and FTIR spectrum (b) of Hranfa's marl

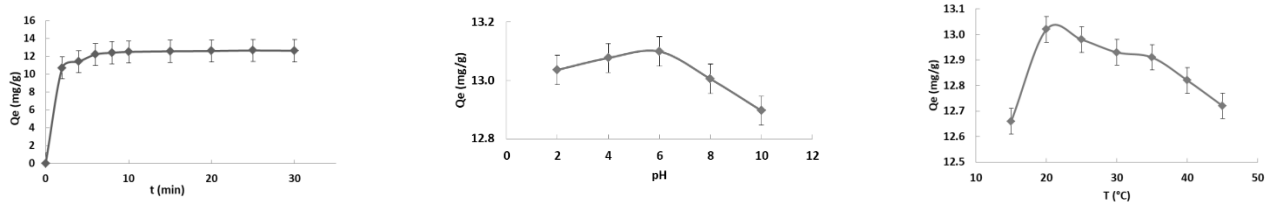

(a) (b) (c)

Fig. 4 Adsorption results in batch conditions for an initial concentration of dye, C_0, equal to 20 mg L^{-1} and an adsorbent dose equal to 1.5 g L^{-1}. (a) Evolution of the adsorbed weight per gram of adsorbent as a function of time. The temperature T was equal to 20 ± 2 °C and the pH of the suspension was equal to 8.2; (b) Effect of pH on the adsorption capacity Q_e. The temperature T was equal to 20 ± 2 °C; (c) Effect of temperature on the adsorption capacity Q_e. The pH was equal 6.

The pH of the solution is a parameter influencing adsorption, since it can affect the surface charge of the adsorbent and also the electric charge and the solubility of the dye present in the aqueous solution (Aguedal *et al.* 2019, Hasnain I *et al.* 2007, Barkat *et al.* 2014, Djafer *et al.* 2014, Aguedal *et al.* 2017, Singh *et al.* 2009). A negative surface charge of adsorbent does not favor the adsorption of dye anions due to electrostatic repulsion (Namasivayam and Kavitha 2002). Although a maximum dye adsorption is observed at pH = 6, the variation of Q_e in the studied pH range is rather limited (Fig. 4b). As previously discussed, Hranfa's marl consists of several phases exhibiting quite different surface chemistries. The silica phases (Quartz and amorphous silica from the diatom frustules) as well as Muscovite have Zero Point of Charge (ZPC) values lower or equal to pH = 2 (Cases 1969, Iler 1979). Their surface charge is thus negative in the studied range of pH. The ZPC of calcium carbonate is close to 9.5 (Huang 1975) and its surface charge is positive for lower pH values. Despite the lack of knowledge on the exact chemical nature of the used industrial dye, taking into account the natural pH of ~7.1 for a dye concentration C_0 of 20 mg L^{-1}, it can be deduced that their acid functions are very weak with pKa values close to 10. The dye molecules are thus mainly neutral (not deprotonated) in the investigated range of pH.

It is known that the increase in temperature influences the mobility of the molecules which promotes the diffusion of the adsorbate through the liquid-solid interface and into the pores of the adsorbent due to the decrease in the viscosity of the solution (Aguedal *et al.* 2019). Figure 4c indicates that the equilibrium uptake decreases with increasing temperature above 20 °C. Such decreased surface activity can be related to the exothermic nature of the phenomenon (Aksu and Karabayir 2008) which has been experimentally confirmed in the present case but will not be detailed in this paper.

The influence of the dose of the adsorbent on the adsorption capacity was studied for different doses ranging from 0.5 to 3 g L^{-1}. Figure 5a shows a maximum of adsorption capacity, with Q_e = 16 mg g^{-1}, when the dose is equal to 1 g L^{-1}. The decrease of Q_e with the increase of adsorbent dose can be explained by a lower dye concentration in the solution at the equilibrium.

According to the literature review, the initial concentration of the pollutant has a significant influence on the retention capacity of the solid support. In order to study its effect, we considered the concentration range from 20 to 180 mg L^{-1} (Fig. 5b). The adsorption capacity increases with the increase in the initial concentration of the dye until reaching a plateau. The adsorption of the marl becomes constant. Linearity for low concentrations shows that the number of free sites, created during the adsorption, remains constant. For large concentrations (≥ 140 mg L^{-1}), the adsorbed amount does not change because the active sites are fully saturated. This same phenomenon has already been reported by other authors using different dyes (Djafer *et al.* 2017, Ho and Ofomaja 2006).

Table 2 gives data selected from the literature concerning the adsorption capacity of different natural materials for different organic dyes and experimental conditions close to those adopted in this study in terms of adsorbent dose and initial concentration of dye. Despite the heterogeneous nature of Hranfa's marl and its low content of clay, its adsorption performance towards organic dye is

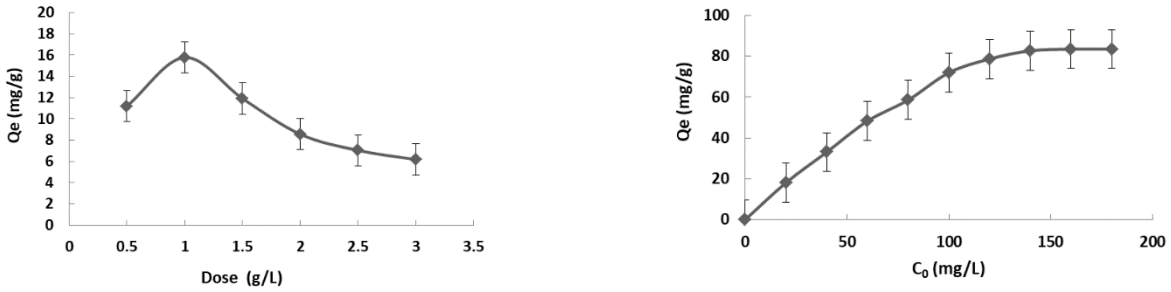

(a) (b)

Fig. 5 Adsorption results in batch conditions for pH = 6 and T = 20 ± 2 °C. (a) Evolution of the adsorption capacity Q_e as a function of the adsorbent dose. C_0 was equal to 20 mg L^{-1}; (b) Effect of the initial concentration of dye, C_0, on the adsorption capacity Q_e. The dose was equal to 1 g L^{-1}.

Table 2 Adsorption capacity of different natural materials for different organic dyes

Adsorbent	Organic dye	Specific surface area (m^2g^{-1})	Adsorption capacity Q_e (mg g^{-1})	Reference
Date stones	Methylene blue (MB)	-	9	Belala *et al.* 2011
Moroccan raw clay from Alhoceima	Methylene blue (MB)	-	19	Sadki *et al.* 2014
Mostaganem's Bentonite	Bemacid Red (E5R)	40	104	Djafer *et al.* 2014
Mostaganem's Bentonite	Bemacid Yellow (E-4G)	110	12	Zahaf *et al.* 2015
Dried activated sludge	Bemacid Red (E5R)	4	38	Djafer *et al.* 2017
Sig's diatomite	Orange bezaktiv	16	18	Aguedal *et al.* 2017
Sig's diatomite	(SRL-150)	21	14	Aguedal *et al.* 2019
Hranfa's marl	Bemacid Red (E-TL)	40	16	This study

comparable, paving the way to possible technological applications. It must be added that the adsorption performance of Hranfa's marl is obviously very low compared to that of recently developed synthetic adsorbents like composite materials based on Metal Oxide Frameworks (MOF) supported on fibrous substrates exhibiting adsorption capacities of few hundred mg g^{-1} and fast adsorption kinetics (Abdelhameed *et al.* 2018 1&2, Abdelhameed and Emam 2019, Emam *et al.* 2019).

3.3 Hybrid process coupling adsorption and membrane separation

To the best of our knowledge, there are very few publications in the literature dealing with a hybrid process directly coupling an adsorption reactor with adsorbents in suspension and a membrane extraction of the purified liquid. Two recent Chinese patents can first be mentioned (Wang *et al.* 2019, Qiu *et al.* 2018). About scientific articles, only two main ones have been identified. The first one (Reddad *et al.* 2004) corresponds to a configuration the closest to that used in our study, with the adsorption of Pb^{2+} ions on polysaccharides contained in a filtration loop equipped with a tubular ceramic microfiltration membrane. The second one (Zheng *et al.* 2013) concerns the extraction of treated water by flat microfiltration or ultrafiltration polymer membranes immersed in an adsorption reactor containing titania nanoparticles for adsorbing viruses.

The first series of experiments conducted with our pilot consisted of dye-free tests to follow the evolution of turbidity, indicative of the presence of suspended solid particles, in different parts of the filtration loop and in the permeate. The obtained results are summarized in Fig. 6a. The measured turbidity becomes rapidly high in the upper part of the adsorption reactor logically leading to a gradual increase in turbidity in the feed of the filtration module, the finest marl particles being entrained via the overflow. On the other hand, the turbidity remains equal to zero in the permeate showing the perfect ability of the used membrane to retain the marl particles inside the loop.

The second series of experiments consisted of marl-free tests to follow the evolution of the dye concentration in the loop and in the permeate (Fig. 6b). During these experiments, the ratio of dye concentration in the permeate, $C_P(t)$, to the concentration of the dye in the loop, $C_L(t)$, was more or less constant and equal to ~ 0.45. Such level of retention is very high considering that the molecular weight of such an organic dye is no more than two thousand grams per mole (Zaharia and Suteu 2012) which is two orders of magnitude less than the molecular weight cut-off of the used membrane with the 0.1 µm pore-sized separative layer. It could be due to dye adsorption at the surface and inside the pores of the membrane which appears as fully colored after use.

The third series of experiments were done with both dye and marl in order to test the performance of the hybrid process. The results shown in Fig. $6c_1$ have to be compared with those obtained without clay (Fig. 6b). The main result to be highlighted is that the concentration of dye in the permeate, $C_P(t)$, is less than 1 mg L^{-1} until 330 minutes after the beginning of the experiment and then starts to rise (Fig.

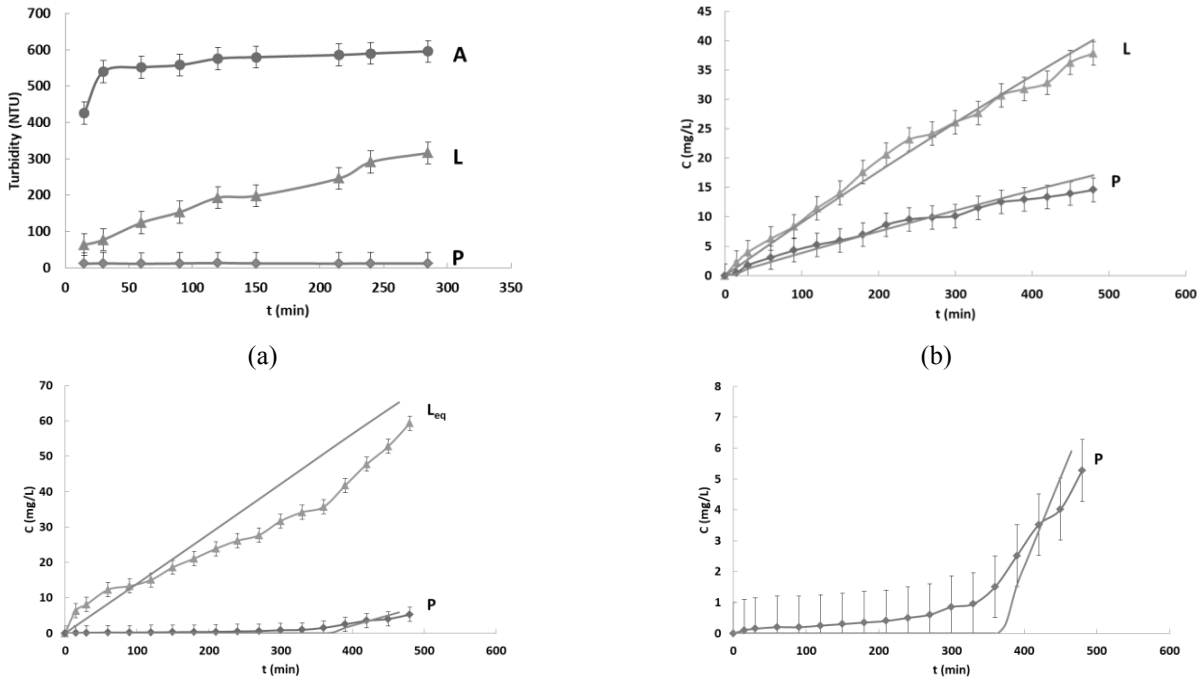

Fig. 6 Evolution of the turbidity and of the dye concentrations during experiments done using the hybrid pilot. (a) Measured turbidity versus time in the upper part of the adsorption reactor (A), in the loop (L) and in the permeate (P) - 80 g of marl in the adsorption reactor and pure water in the feed tank (no dye) – in flow = out flow = 25 mL min^{-1}. (b) Measured (symbols) and calculated (continuous lines) curves of dye concentrations in the the loop $C_L(t)$ (L), in the permeate $C_P(t)$ (P) - no marl in the adsorption reactor and 80 mg L^{-1} of dye in the feed tank– in flow = 22 mL min^{-1}, out flow = 23 mL min^{-1} – calculated curves drawn assuming a constant ratio $C_P(t)/C_L(t) = 0.45$. (c_1) Measured (symbols) and calculated (continuous lines) curves of dye concentrations in the the loop (overall concentration, i.e. free and adsorbed) $C_{L,eq}(t)$ (L_{eq}), in the permeate $C_P(t)$ (P) – 80 g of marl in the adsorption reactor and 110 mg L^{-1} of dye in the feed tank – in flow = 24 mL min^{-1}, out flow = 25 mL min^{-1} – calculated curves drawn assuming a constant ratio $C_P(t)/ C_L(t) = 0.45$. (c_2) Figure derived from figure $6c_1$, with only the measured (symbols) and calculated (continuous lines) curves of dye concentrations in the permeate $C_P(t)$ (P).

$6c_2$). This experimental breakthrough curve is in fact rather close to the ideal one considering that no dye will cross the membrane as long as the adsorbent is not saturated (full and instantaneous adsorption and no free dye in the loop before adsorbent saturation). The simulated ideal curves calculated using an adsorption capacity Q_e equal to 12 mg g^{-1} (defined from Fig. 5a) are also drawn in Figs. $6c_1$ and $6c_2$. In ideal conditions, the time required for having free dye in loop and thus able to cross the membrane is 364 minutes.

The overall concentration of dye in the loop taking into account the free and adsorbed parts, $C_{L,eq}(t)$, has been measured after filtration through a 4-micron filter paper and rinsing the filtrate with the pure water added for diluting the solutions before absorbance measurements. It can be seen in Fig. $6c_1$ that the measured values of $C_{L,eq}(t)$ are lower those calculated from in and out flows in the loop. It can be explained by an incomplete release of the dye physisorbed on the filtrate, leading to an underestimation of the overall concentration of dye in the loop.

It must also be mentioned that during all the set of experiments, the permeate flow under the selected transmembrane pressure, i.e. 0.5 bar is remained almost the same taking into account the uncertainty of the measurements (from 23 to 25 mL min^{-1}). By way of consequence no cleaning treatment was required. The measured flow corresponds to a water permeance of 380-420 L m^{-2} h^{-1} bar^{-1} in full agreement with the value expected for the used microfiltration membrane. This shows that no significant fouling occurred, caused by the presence of the adsorbate and/or the adsorbent in the feed. This also indicates that the presence of the marl particles in suspension in the loop did not induce a notable degradation by abrasion of the top layer of the membrane.

One issue before a possible technological development of this hybrid process is the management of the adsorbent replacement before its full saturation. The initial approach was to stop the stirring of adsorption tank in order to enable a fast sedimentation of the large adsorbent particles. However due to the brittleness of these large aggregates of marl exhibiting a heterogeneous microstructure and to their easy attrition in suspension giving rise to finer particles, such a procedure is not possible. A complete emptying of the treatment loop must be considered.

4. Conclusions

This work was focused on the use of low cost and abundant Hranfa's marl as adsorbent for the removal of an industrial dye from textile wastewater and on its

implementation in a hybrid process coupling adsorption to membrane separation.

Hranfa's marl shows a great diversity of morphologies: rounded particles, platelets, needles and also entities with architectural porosity similar to frustules (silica shell) of diatoms and low sedimentation velocities resulting from the easy fragmentation/attrition of larger soft aggregates selected by sieving after crushing.

The four main crystalline phases are, in descending order of importance, Calcite, Quartz, calcium magnesium iron carbonate and a phyllosilicate phase identified as being Muscovite. The adsorption capacity of the Bimacid Red E-TL on Hranfa's marl, in usual experimental conditions, is equal to 16 mg g^{-1}. This adsorption capacity is comparable to that of previously tested natural materials paving the way to possible technological applications.

Experiments done using a hybrid pilot unit coupling adsorption and membrane filtration validate the interest of this approach with a breakthrough curve for the dye concentration in the water outgoing from the treatment unit rather close to the ideal one considering that no dye will cross the membrane as long as the adsorbent is not saturated (full and instantaneous adsorption and no free dye in the loop before adsorbent saturation). The implemented pilot is simple to use and robust. No significant fouling or abrasion of the used ceramic membrane has been observed during all the set of performed experiments.

Acknowledgments

The authors warmly thank D. Cot and B. Ribière (IEM) for SEM and EDX analyses, A. El Manssouri (IEM) for specific surface area measurements, D. Granier (Réseau RX and gamma ICGM) for DRX analyses, F.B. Henni Chebra and F. Guitarni (University of Chlef) for FTIR and chemical analyses. They also thank the Algerian and the French Ministries of Higher Education and Research for their financial support.

References

Abdelhameed, R. M., el-deib, H. R., El-Dars, F. M. S. E., Ahmed, H.B. and Emam, H.E. (2018), "Applicable Strategy for Removing Liquid Fuel Nitrogenated Contaminants Using MIL-53-NH_2@Natural Fabric Composites", *Industrial Eng. Chem. Res.,* **57**(44), 15054-15065. https://doi.org/10.1021/acs.iecr.8b03936.

Abdelhameed, R. M., El-Zawahry, M. and Emam, H.E. (2018), "Efficient removal of organophosphorus pesticides from wastewater using polyethylenimine-modified fabrics", *Polymer,* **155**, 225-234. https://doi.org/10.1016/j.polymer.2018.09.030.

Abdelhameed, R. M. and Emam, H. E. (2019), "Design of ZIF(Co & Zn)@wool composite for efficient removal of pharmaceutical intermediate from wastewater", *J. Colloid Interface Sci.,* **552**, 494-505. https://doi.org/10.1016/j.jcis.2019.05.077.

Aguedal, H., Hentit H., Merouani, D., Iddou, A., Šiškins, and Jumas, J. (2017), "Improvement of the sorption characteristics of diatomite by heat treatment", *Key Eng. Mater.,***721**, 111-116. https://doi.org/10.4028/www.scientific.net/KEM.721.111.

Aguedal, H., Iddou, A., Azziz, A., Shishkin, A., Ločs, J. and Juhna, T. (2019), "Effect of thermal regeneration of diatomite adsorbent on its efficacity for removal of dye from water", *Int. J. Environ. Sci. Technol.,* **16**(1), 113-124. https://doi.org/10.1007/s13762-018-1647-5.

Aksu, Z. and Karabayır, G. (2008), "Comparison of biosorption properties of different kinds of fungi for the removal of Gryfalan Black RL metal-complex dye", *Bioresource Technol.,* **99**, 7730–7741. https://doi.org/10.1016/j.biortech.2008.01.056

Bagane, M. and Guiza, S. (2000), "Elimination d'un colorant des effluents de l'industrie textile par adsorption", *Ann. Chim. Sci. Mat*., **25**, 615-626.

Baghriche, O., Djebbar, K. and Sehili, T. (2008), "Etude cinétique de l'adsorption d'un colorant cationique (vert de méthyle) sur du charbon actif en milieu aqueux", *Sciences et Technologie,* **27**, 57-62.

Barkat, M., Chegrouche, S., Mellah, A., Bensmain, B., Nibou, D. and Boufatit, M. (2014), "Application of algerian bentonite in the removal of cadmium (II) and chromium (VI) from aqueous solutions", *J. Surface Eng. Mater. Adv. Technol.,* **4**(4), 210-226. https://doi.org/10.4236/jsemat.2014.44024.

Belala, Z., Jeguirim, M., Belhachemi, M., Addoun, F. and Trouvé, G. (2011), "Biosorption of basic dye from aqueous solutions by date stones and palm-trees waste: Kinetic, equilibrium and thermodynamic studies", *Desalination,* **271**, 80-87. https://dx.doi.org/10.1016/j.desal.2010.12.009.

Cases, J. M. (1969), "Zero point charge and structure of silicates", *Journal de Chimie Physique et de Physico-Chimie Biologique,* **66**(10), 1602-1611. https://doi.org/10.1051/jcp/196966s21602.

Charumathi, D. and Das, N. (2012), "Packed bed column studies for the removal of synthetic dyes from textile wastewater using immobilised dead C. Tropicalis", *Desalination,* **285**, 22–30. https://dx.doi.org/10.1016/j.desal.2011.09.023.

Cimino, G., Passerini, A. and Toscano, G. (2000), "Removal of toxic cations and Cr(VI) from aqueous solution by hazelnut shell", *Water Research,* **34**(11), 2955-2962. https://dx.doi.org/10.1016/S0043-1354(00)00048-8.

CHT Smart Chemistry with Character (2019), The CHT Group; Tübingen, Germany, https://www.cht.com.

Dali-Youcef, Z., Bouabdasselem, H. and Bettahar, N. (2006), "Élimination des composés organiques par des argiles locales", *Comptes Rendus Chimie,* **9**(10), 1295-1300. https://doi.org/10.1016/j.crci.2006.05.001.

Dinçer, A.R., Güneş, Y. and Karakaya, N. (2007), "Coal-based bottom ash (CBBA) waste material as adsorbent for removal of textile dyestuffs from aqueous solution", *J. Hazardous Mater.,* **141**(3), 529-535. https://doi.org/10.1016/j.jhazmat.2006.07.064.

Djafer, A., Kouadri Moustefai, S., Iddou, A. and Si Al,i B. (2014), "Study of bimacid dye removal from aqueous solution: A comparative study between adsorption on pozzolana, bentonite, and biosorption on immobilized anaerobic sulfate-reducer cells", *Desalination Water Treat.,* **52**(40-42), 7723-7732. https://doi.org/10.1080/19443994.2013.833866.

Djafer, A., Djafer, L., Maimoun, B. and Ayral, A. (2017), "Reuse of waste activated sludge for textile dyeing wastewater treatment by biosorption: performance optimization and comparison", *Water Environ. J.,* **31**(1), 105-112. https://doi.org/10.1111/wej.12218.

Emam, H. E., Ahmed H. B., El-Deib H. R., El-Dars F. M.S.E. and Abdelhameed R.M. (2019), "Non-invasive route for desulfurization of fuel using infrared-assisted MIL-53(Al)-NH2 containing fabric", *J. Colloid Interface Sci.,* **556**, 193-205. https://doi.org/10.1016/j.jcis.2019.08.051.

Flörke, M., Kynast, E., Bärlund, I., Eisner, S., Wimmera, F. and Alcamo, J. (2013), "Domestic and industrial water uses of the past 60 years as a mirror of socio-economic development: global simulation study", *Glob. Environ. Change.,* **23**(1), 144–156. https://doi.org/10.1016/j.gloenvcha.2012.10.018.

Fu, Y. and Viraraghavan, T. (2001), "Fungal decolorization of dye wastewaters: A review", *Bioresour. Technol.,* **79**, 251–262.

https://doi.org/10.1016/S0960-8524(01)00028-1.
Hasnain, Isa M., Lang, L.S., Asaari, F.A.H., Aziz, H.A., Azam Ramli, N. and Dhas, J.P.A. (2007), "Low cost removal of disperse dyes from aqueous solution using palm ash", *Dyes Pigm.,* **74**(2), 446-453. http://dx.doi.org/10.1016/j.dyepig.2006.02.025.
Ho, Y. and Ofomaja, A.E. (2006), "Biosorption thermodynamics of cadmium on coconut copra mealas biosorbent", *J. Biochem. Eng.,* **30**, 117-123. https://doi:10.1016/j.bej.2006.02.012.
Huang, C.P. (1975), "Adsorption of Tryptophan onto Calcium Carbonate Surface", *Environ. Lett.,* **9**(1), 7-17. https://doi.org/10.1080/00139307509437452.
Iler, R.K., (1979), *The Chemistry of Silica: Solubility, Polymerization, Colloid and Surface Properties and Biochemistry,* John Wiley and Son, Chichester, United Kingdom.
Kumar, S., Zafar, M., Prajapati, J.K., Kumar, S. and Kannepalli, S., (2011), "Modeling studies on simultaneous adsorption of phenol andresorcinol onto granular activated carbon from simulated aqueous solution", *J. Hazard. Mater.,* **185**, 287–294. https://doi.org/10.1016/j.jhazmat.2010.09.032.
Namasivayam, C. and Kavitha, D., (2002), "Removal of congo red from water by adsorption on to activated carbon prepared from coirpith, an agricultural solid waste", *Dyes Pigm.* **54**, 47–58. http://dx.doi.org/10.1016/S0143-7208(02)00025-6.
Perineau, F., Molinier, J. and Gazet, A., (1983), "Adsorption of ionic dyes on wool carbonizing waste", *Wat. Res.,* **17**(5), 559-67.
Qiu, L., Cheng, R., Song, Q.,Qiu, Q., Wang, Y., Wang, Y., Han, Q. and Hu, M. (2018), "A kind of integrated device for advanced treatment of industrial wastewater by granular active carbon coupling ceramic membrane and use method thereof", *Faming Zhuanli Shenqing*, CN 108101266 A 20180601.
Reddad, Z., Gérentes, C., Andrès, Y. and LeCloirec, P. (2004), "Lead removal by a natural polysaccharide in membrane reactors", *Water Sc. Technol.,* **49**(1), 163-170. https://doi.org/10.2166/wst.2004.0048.
Sadki, H., Ziat, K., Saidi, M. (2014), "Adsorption d'un colorant cationique d'un milieu aqueux sur une argile locale activée", *J. Mater. Environ. Sci.* **5**, 2060-2065.
Singh, V., Sharma, A.K., Tripathi, D.N., Sanghi, R. (2009), "Poly(methylmethacrylate) grafted chitosan: An efficient adsorbent for anionic azo dyes", *J. Hazard. Mater.* **161**, 955–966. https://doi.org/10.1016/j.jhazmat.2008.04.096.
Vaughan, T., Seo, C.W., Marschall, W.E. (2001), "Removal of selected metal ions from aqueous solution using modified corncobs", *Bioresour. Technol.* **78**, 133-139. https://doi.org/10.1016/S0960-8524(01)00007-4.
Wang, J., Song, H., Chen, S., He, J. and Ji, C. (2019), "Adsorption-membrane separation coupling device for removing antibiotics in wastewater and wastewater treatment method", *Faming Zhuanli Shenqing*, CN 109867372 A 20190611.
Yaneva, Z. and Koumanova, B. (2006), "Comparative modelling of mono- and dinitrophenols sorption on yellow bentonite from aqueous solutions", *J. Colloid Interface Sci.,* **293**, 303-311. https://doi.org/10.1016/j.jcis.2005.06.069.
Yang, Y., Ladisch, C. and Ladisch, M. R. (1988), "Cellulosic adsorbents for treating textile mill effluents", *Enzym. Microb. Tech.,* **10**, 632-636. https://doi.org/10.1016/0141-0229(88)90111-1.
Zahaf, F., Dali, N., Marouf, R. and Ouadjenia, F. (2015), "Removal of a textile dye by pillared clay", *J. Chem. Environ. Eng.*, **6**(1), 11-14.
Zaharia, C. and Suteu, D. (2012), "Textile organic dyes - characteristics, polluting effects and separation/elimination procedures from industrial effluents - A critical overview", *Organic Pollutants Ten Years after the Stockholm Convention: Environmental and Analytical Update,* InTech, Rijeka, Croatia. 55-86.
Zheng, X., Chen, D., Wang, Z., Lei, Y. and Cheng, R. (2013), "Nano-TiO_2 membrane adsorption reactor (MAR) for virus removal in drinking water", *Chem. Eng. J.,* **230**, 180-187. https://doi.org/10.1016/j.cej.2013.06.069.

ED